BIOCHEMISTRY
including biophysical chemistry & molecular biology

Article

pubs.acs.org/biochemistry

Different Modes of Carbon Monoxide Binding to Acetyl-CoA Synthase and the Role of a Conserved Phenylalanine in the Coordination Environment of Nickel

Simonida Gencic,[†] Kayla Kelly,[‡,∥] Selamawit Ghebreamlak,[§] Evert C. Duin,[§] and David A. Grahame*[,†]

[†]Department of Biochemistry and Molecular Biology, Uniformed Services University of the Health Sciences, Bethesda, Maryland 20814, United States

[‡]Holton-Arms School, Bethesda, Maryland 20817, United States

[§]Department of Chemistry and Biochemistry, Auburn University, Auburn, Alabama 36849, United States

ABSTRACT: Acetyl-CoA synthase (ACS) catalyzes the reversible condensation of CO and CH_3 units at a unique Ni−Fe cluster, the A cluster, to form an acetyl-Ni intermediate that subsequently reacts with CoA to produce acetyl-CoA. ACS is a component of the multienzyme complex acetyl-CoA decarbonylase/synthase (ACDS) in Archaea and CO dehydrogenase/ACS (CODH/ACS) in bacteria; in both systems, intraprotein CO channeling takes place between the CODH and ACS active sites. Previous studies indicated that protein conformational changes control the chemical reactivity of the A cluster and suggested the involvement of a conserved Phe residue that moves concomitantly into and out of the coordination environment of Ni. Herein, steady-state rate measurements in which both CO and CH_3-corrinoid are varied, and rapid methylation reactions of the ACDS β subunit, measured by stopped-flow methods, provide a kinetic model for acetyl-CoA synthesis that includes a description of the inhibitory effects of CO explained by competition of CO and CH_3 for the same form of the enzyme. Electron paramagnetic resonance titrations revealed that the formation of a paramagnetic Ni^+-CO species does not match the kinetics of CO interaction as a substrate but instead correlates well with an inhibited state of the enzyme, which requires revision of previous models that postulate that this species is an intermediate. Characterization of the β subunit F195A variant showed markedly increased substrate reactivity with CO, which provides biochemical functional evidence of steric shielding of the CO substrate interaction site by the phenyl group side chain. The phenyl group also likely enhances the nucleophilicity of the Ni center to facilitate CH_3 group transfer. A model was developed for how the catalytic properties of the A cluster are optimized by linking conformational changes to a repositionable aromatic shield able to modulate the nucleophilicity of Ni, sterically select the most productive order of substrate addition, and overcome intrinsic inhibition by CO.

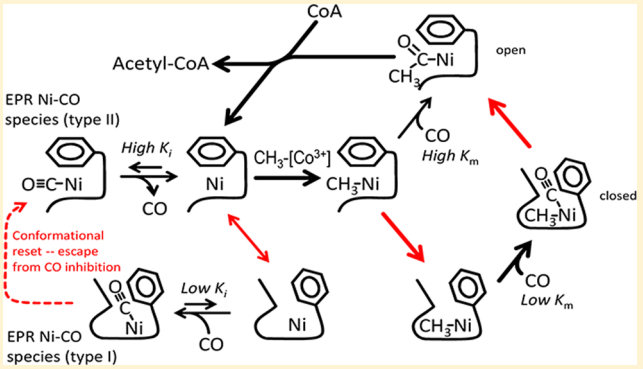

Acetyl-CoA synthase (ACS) catalyzes the synthesis and cleavage of the acetyl C−C and C−S bonds of acetyl-CoA in anaerobic bacteria and in methanogens and other species of Archaea. The enzyme contains an unusual active site metal cluster, designated the A cluster, that consists of a binuclear Ni Ni center bridged to an $[Fe_4S_4]$ cluster.[1−3] In bacteria, ACS is present as an 82 kDa α subunit usually found in association with CO dehydrogenase (CODH) β subunits in a 310 kDa $\alpha_2\beta_2$ heterotetrameric enzyme designated CODH/ACS. In Archaea, ACS comprises the 53 kDa β subunit of an ∼2000 kDa multienzyme complex with a probable oligomeric structure of $(\alpha_2\varepsilon_2)_4\beta_8(\gamma\delta)_8$ designated acetyl-CoA decarbonylase/synthase (ACDS). As indicated in Scheme 1, a substantial portion of the sequence of the archaeal ACDS β subunit (residues 3−398 in *Methanosarcina thermophila*) is conserved in common with bacteria (residues 319−724 in the ACS α subunit in *Moorella thermoacetica*), in a region designated pfam03598 in the NCBI conserved domain database.[4] This region encompasses the central domain and C-terminal domain, which harbors the A cluster. The first ∼320 amino acid residues of the ACS α subunit form a large N-terminal domain that makes contact with both the central and C-terminal regions. In the CODH/ACS heterotetramer, neither the central nor the C-terminal region directly contacts the CODH subunits because the ACS N-terminal domain intervenes. A tunnel extending from the site of CO production at the C cluster in CODH through the N-terminal domain allows for the intraprotein transfer of CO to the A cluster site for incorporation into acetyl-CoA.

The crystallographic structures of open and closed conformational states of bacterial ACS suggest that the N-terminal

Received: December 17, 2012
Revised: February 7, 2013
Published: February 8, 2013

Scheme 1. Schematic Alignment of Acetyl-CoA Synthase Subunits[a]

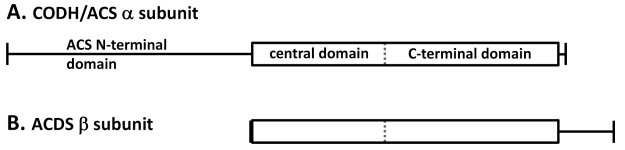

[a](A) Bacterial α subunit (CODH/ACS from *Moorella thermoacetica*, 729 amino acids). (B) Archaeal β subunit (ACDS from *Methanosarcina thermophila*, 472 amino acids). Boxed areas indicate the conserved regions.

domain regulates the transfer of CO by alternately allowing or blocking access through the tunnel.[2,5] In the open conformation, the A cluster experiences an increased level of solvent exposure because of fewer contacts between the N-terminal domain and both the central and C-terminal domains. In the same conformation, the tunnel becomes obstructed at a location within the N-terminal domain. In addition, a strictly conserved phenylalanine side chain located in the C-terminal domain (Phe 195 in the *Methanosarcina* ACDS β subunit, which corresponds to Phe 516 in the *Moorella* subunit) adopts a position that shields the approach to the axial coordination site of the reactive Ni atom (designated Ni_p, because it is the Ni atom proximal to the $[Fe_4S_4]$ cluster).[3,5] Scheme 2 shows the location of the conserved phenylalanine side chain and illustrates its potential to hinder access to Ni_p in the open form of the α subunit in the CODH/ACS enzyme from *Moorella*.

A comparison of kinetic and electron paramagnetic resonance (EPR) spectroscopic properties of three different ACS protein forms indicates that protein conformational changes have a direct effect on the stability of the enzyme Ni-acetyl intermediate.[6] Alterations in the Ni_p coordination environment are postulated to promote C−C bond fragmentation in a process that is strictly dependent on changes in the conformational state that occur in proceeding from the open to the closed form. In essence, the direct conformational control over acetyl C−C bond fragmentation, along with the containment of CO in the tunnel, forms the basis for tight coupling of the decarbonylation reaction on ACS with the transfer and oxidation of CO to CO_2 by CODH. The role of the reorientation of Phe 195 (ACDS) in this process is largely unexplored. Herein, we report kinetic and EPR spectroscopic studies that support a mechanism that accounts for different modes of interaction of CO with the ACDS β subunit, acting both as a substrate and as an inhibitor. A comparison of the properties of the wild-type β subunit and F195A variant indicates that the Phe 195 phenyl group exerts both steric and electronic effects on the Ni_p site. The kinetic model suggests that protein conformational changes are involved in the regulation of the interaction of CO with the enzyme and are employed to overcome steps in the organometallic mechanism that otherwise lead to substrate inhibition.

MATERIALS AND METHODS

General Reagents and Materials. All reagents purchased from commercial sources were of the highest purity grade offered. Coenzyme A, disodium salt [>96%, high-performance liquid chromatography (HPLC), Fluka BioChemika], was from Sigma. All anaerobic procedures were conducted inside a Coy-type anaerobic chamber maintained with an atmosphere of N_2

Scheme 2. Repositioning of the Phenyl Side Chain of Conserved Phe 512 (Phe 195 in the ACDS β subunit) in the Open and Closed Forms of the CODH/ACS α Subunit from *M. thermoacetica*[a]

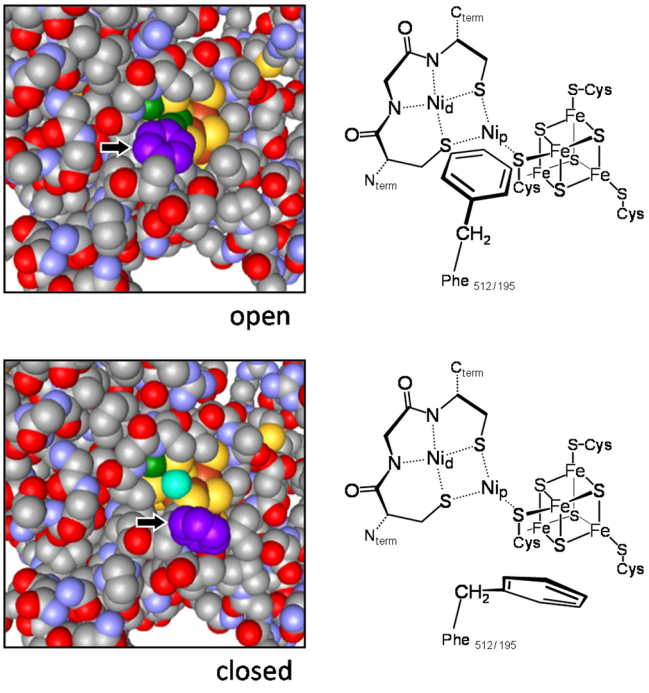

[a]On the left, portions of the α subunit C-terminal domain are shown in space filling mode with the N-terminal domain cut away to allow a view of the A cluster. The phenyl ring (magenta) is indicated by the arrow. The A cluster proximal metal atom is shielded in the top panel but is visible in the bottom panel as the light green atom in the center of the field. On the right, the corresponding A cluster bonding arrangements are drawn in similar orientations. The Ni atom proximal to the $[Fe_4S_4]$ center, Ni_p, is coordinated by three μ-cysteine thiolate sulfur atoms; one of them forms a bridge to Fe in the $[Fe_4S_4]$ cluster, and the other two share coordination with the distal Ni, Ni_d. Condensation of CO and CH_3 groups (not shown) bound to Ni_p takes place to form an acetyl-Ni intermediate,[8] from which the acetyl group is subsequently rapidly transferred to CoA to form acetyl-CoA. Data are from Protein Data Bank entry 1OAO by Darnault et al.[2]

containing 1−3% H_2; levels of O_2 were in the range of 0.5−2 ppm, as monitored by a Teledyne model 3190 trace oxygen analyzer. High-purity CO gas was from Matheson (research purity grade, 99.998%, <0.5 ppm O_2). Nitrogen gas for CO/N_2 mixtures was standard high-purity grade that had been further passed through an Oxiclear (Labclear) gas purifier unit located inside the anaerobic chamber to provide an N_2 source with <0.1 ppm O_2. Titanium (III) nitrilotriacetate (Ti NTA) stock solution (approximately 174 mM) was prepared fresh daily by adding 72.5 μL of anaerobic 30% (w/w) titanium(III) chloride in 2 N HCl reagent (Acros Organics) to 1.0 mL of an anaerobic solution containing 0.275 M nitrilotriacetate disodium salt and 0.5 M Tris-HCl (pH 8.0). Further dilution with water provided a 1.72 mM Ti^{3+} working solution for direct additions to enzyme reaction mixtures. Ti citrate stock solutions were prepared fresh by adding 1 volume of 30% (w/w) $TiCl_3$ reagent to 19 volumes of anaerobic 0.5 M trisodium citrate; further dilution with MOPS buffer (pH 8.0) provided a working solution of 11 mM Ti^{3+} and 30 mM MOPS (pH 6.6).

Methylcobinamide was prepared from methylcobalamin by the method developed in the laboratory of K. L. Brown,[7] as

described previously,[8] with modifications to chromatographic procedures that improved overall yield and final purity. Instead of elution of the crude product from the series of five Sep-Pak C18 cartridges (Waters) with 50% methanol immediately after the water wash, the cartridge chain was first further washed with 30 mL of 20 mM ammonium acetate (pH 4.8), and thereafter, fractions were collected while solutions of increasing methanol concentration were applied, consisting of 22 mL of 10%, 10 mL of 20%, 22 mL of 40%, and a final 15 mL of 60% methanol prepared in the same ammonium acetate buffer. Cation exchange chromatography was performed on the entire batch of the desalted material using a 25 mL column of SP Sepharose Fast Flow (GE Healthcare) instead of smaller batches, which was done previously with a 5 mL Econo-Pac High S cartridge (Bio-Rad). Final desalting employed a second gradient elution from a second series of Sep-Pak C18 cartridges. Overall, the procedure gave a 32% yield of methylcobinamide at 98−99% purity (monitored by HPLC at 250 nm).

Construction, Heterologous Expression, and Purification of the Wild-Type ACDS β Subunit and F195A Form. The ACDS β subunit from *M. thermophila* TM-1 was expressed in anaerobically grown *Escherichia coli* as a 397-amino acid protein lacking 75 amino acids at the C-terminus, as described previously.[9] The F195A mutation was introduced using the QuikChange site-directed mutagenesis kit (Stratagene/Agilent) according to the manufacturer's instructions and confirmed by DNA sequencing. Protein purification of the nontagged proteins was performed as described previously;[8] supernatants obtained following anaerobic French pressure cell lysis of resuspended cell pastes were subjected first to chromatography on Q-Sepharose Fast Flow (GE Healthcare) and then to chromatography on a Superose 12 HR 10/30 gel filtration column (GE Healthcare). Nickel reconstitution of the purified proteins was carried out as described previously,[6] except that for EPR samples, following overnight incubation with 0.15 mM $NiCl_2$ and 50 mM MOPS (pH 7.7), the Ni-reconstituted enzyme was subjected to a final step of gel filtration on Superose 12. Thereafter, concentration and final diafiltration with 20 mM MOPS buffer (pH 7.7) were performed using a YM-30 ultrafiltration membrane in a 10 mL Amicon stirred cell (EMD Millipore).

Acetyl-CoA Synthesis Reactions. Assays for acetyl-CoA synthesis from CoA, methylcobinamide, and CO were conducted as described previously, with provisions to vary the concentration of dissolved CO by use of a simple mounted balloon-type device to produce and deliver different gas mixtures of CO in N_2 to sealed 1.5 mL tubes containing the 100 μL reaction mixtures.[6,10] All steps were performed inside the anaerobic chamber. The enzymes were preincubated at pH 7.2 and 25 °C in the presence of 34 μM Ti NTA with the indicated concentrations of methylcobinamide and CO gas mixtures for 5 min before addition of CoA (final concentration of 120 mM) to initiate the reaction. Reversed phase HPLC analysis was used to quantify acetyl-CoA and CoA in aliquots removed over time, and initial rates were obtained from first-order fits of fractional conversion versus time, as previously described.[6,10]

Stopped-Flow Measurements. Rapid kinetic assays were conducted with an SFA-20 accessory (TgK Scientific), after allowing all components of the device to equilibrate for more than 1 week inside the anaerobic chamber. An HP 8452A diode array spectrophotometer was used to collect spectral data at 0.1 s intervals over the range of 384−422 nm. The fidelity of the system was verified by use of ferricyanide/ascorbate reduction reactions.[11] One syringe contained 45.2 μM ACDS β subunit reduced with 0.4 mM Ti NTA in 50 mM MOPS (pH 7.7). The other syringe contained either 118 or 236 μM methylcobinamide in the same buffer. The data were numerically fit to the following rate expression:

$$\mathrm{d[cob(I)inamide]}/\mathrm{d}t = k'[\text{methylcobinamide}][\text{enzyme}] + k_p[\text{methylcobinamide}]$$

where k' is the second-order rate constant for the reaction of the enzyme with methylcobinamide and k_p is a first-order rate constant used to approximate the extent of photolysis of the methylcobinamide at time t due to light from the unfiltered deuterium lamp in the spectrophotometer. The cob(I)inamide concentration was obtained from the change in the absorbance function $A_{388-420}$ using a $\Delta\varepsilon$ value of 23.5 mM^{-1} for conversion of methylcobinamide to cob(I)inamide determined in separate experiments.

EPR Spectroscopic Analyses. Samples for EPR spectroscopy were prepared under strictly anaerobic conditions by equilibration of solutions containing approximately 100 μM enzyme and 0.5 mM Ti citrate with different gas mixtures in which the composition of CO in N_2 was varied. Protein samples, 200 μL in 20 mM MOPS buffer (pH 7.7), were first mixed with 10 μL of 11 mM Ti citrate, and after 2 min, the mixture was injected through a butyl rubber stopper into a 2 mL conical glass vial (Kimax-Kimble Chase) prepurged with the corresponding CO/N_2 gas mixture using the gas mixing device described above. The vial was set up as part of a closed system that included a 25 mL syringe and calibrated 0−60 psi pressure gauge for adjustment of the total gas pressure. Also part of the system was a sliding cannula inserted through the vial stopper connected to a length of 0.67 mm (inside diameter) × 1.22 mm (outside diameter) polyethylene tubing for the subsequent transfer of the reaction mixture to the bottom of a stoppered 3 mm (inside diameter) quartz EPR tube. (Because efficient gas equilibration is required, incubation of a narrow column of the enzyme solution directly in EPR tubes is precluded, so the conical vial system, with an ∼11 times larger surface:volume ratio, was used for efficient gas exchange during incubation.) The entire system was thoroughly flushed with a CO/N_2 gas mixture prior to introduction of the protein. Immediately after injection of the reduced enzyme, the pressure was adjusted to values from 2.05 to 2.15 atm total (1.05 to 1.15 atm overpressure), and incubation was conducted with gentle agitation at room temperature for 15 min. Thereafter, the sample was transferred to the EPR tube while the total pressure in the system was kept essentially constant. To initiate the transfer, the cannula was positioned at the bottom of the vial and a small volume of gas was removed from the headspace of the EPR tube using an attached 1 mL gastight Hamilton syringe; thereby, a small pressure difference was created between the vial and EPR tube sufficient to cause the sample to flow from the vial into the EPR tube via the cannula and connecting tubing. After the sample had been frozen in liquid N_2, the pressure in the apparatus was released, allowing excess CO to vent outside the anaerobic chamber into a fume hood, and the EPR tube was disconnected from the system. The CO partial pressure was determined by multiplying the volume fraction of CO in the gas mixture by the total pressure, and the CO concentration was obtained from the partial pressure

dx.doi.org/10.1021/bi3016718 | *Biochemistry* 2013, 52, 1705−1716

assuming 0.956 mM/atm calculated using the α value for CO solubility in water at 25 °C.[12]

EPR spectra were recorded at X-band frequency (9 GHz) with a Bruker EMX spectrometer fitted with the ER-4119-HS high-sensitivity perpendicular mode cavity. The sample temperature was kept at 70 K with an Oxford Instruments ESR 900 flow cryostat with an ITC4 temperature controller. Spin quantification was conducted under nonsaturating conditions using 0.5, 1.0, and 10 mM copper perchlorate standards prepared from $CuSO_4$ dissolved in 10 mM HCl and 2 M $NaClO_4$.

RESULTS

Steady-State Kinetic Model for the Acetyl-CoA Synthase Overall Reaction. Although a number of kinetic experiments with ACS enzymes have been reported previously, e.g., on the characterization of partial reactions such as [1-^{14}C]acetyl-CoA/CO exchange, methyl transfer, and acetyl transfer reactions,[6,13−20] a steady-state kinetic analysis of the overall reaction in which both carbonyl and methyl donor substrate concentrations were varied has not been described. Strong inhibitory effects of CO on the overall reaction of acetyl-CoA synthesis have been observed previously for both CODH/ACS and the isolated bacterial ACS subunit.[6,16] However, the available data were insufficient to determine whether CO also inhibits the enzyme in its conformationally open state, such as with the ACDS β subunit and the N-terminally truncated bacterial enzyme $ACS_{Ch}\Delta N$ (enzyme forms that show apparent K_m^{CO} values much higher than that of the full-length ACS). Therefore, additional acetyl-CoA synthase reactions were conducted with the ACDS β subunit over a wider range of CO concentrations. The results, shown in Figure 1 (empty symbols), indicate that CO inhibition is also a characteristic of the open-only form of the enzyme.

Variation of the concentration of CH_3 donor substrate methylcobinamide was then conducted at different fixed levels of CO, as shown in Figure 2. The kinetic pattern was consistent

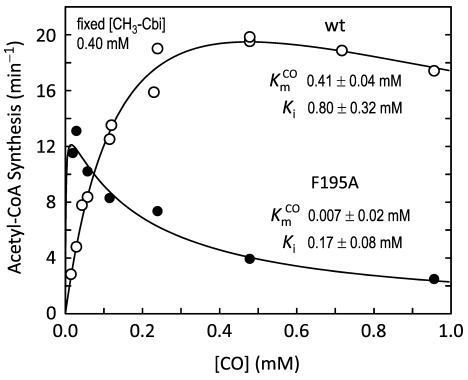

Figure 1. CO substrate inhibition of the ACDS β subunit and F195A variant. Acetyl-CoA synthesis reactions were performed at different levels of dissolved CO with fixed concentrations of methylcobinamide, 0.40 mM, and CoA, 0.12 mM, as described in Materials and Methods. Best-fit lines are drawn to the velocity equation for kinetic mechanism I (inverse of the form given in Scheme 3) using the value for V_{max} determined in Figure 2 as a nonadjustable constant. The $K_m^{CH_3}$ values provided by these fits are 0.6 ± 0.1 and 1.9 ± 0.5 mM for the wild type and F195A variant, respectively. Values for K_m^{CO} and K_i are as indicated. The reaction rate is expressed as turnover number, mol acetyl-CoA formed per mol enzyme per min.

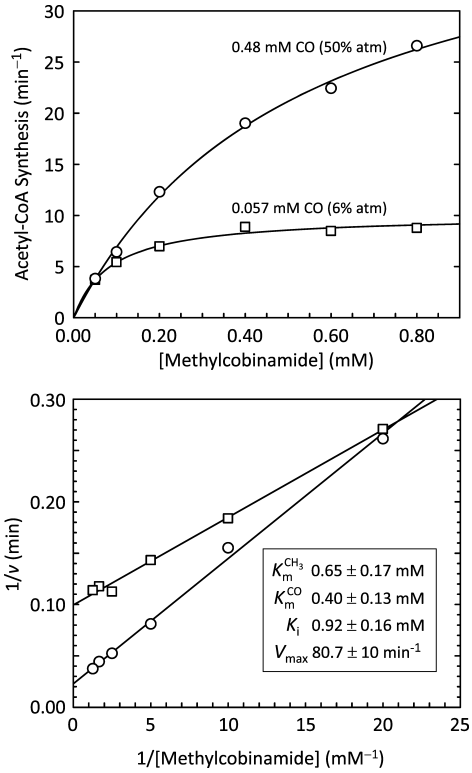

Figure 2. Steady-state kinetic pattern for acetyl-CoA synthase. Rates of acetyl-CoA synthesis by the ACDS β subunit were measured at different levels of methylcobinamide in reaction mixtures equilibrated with a gas phase containing 6 or 50% CO in a balance of N_2, corresponding to dissolved CO concentrations of 0.0574 and 0.478 mM. Standard v vs [S] and double-reciprocal plots are shown. Rate data at 50% CO were taken from ref 8. V_{max} expressed in units of turnover number is equivalent to k_{cat} for the reaction. The lines are drawn according to the fit of all data to the model given in Scheme 3 (mechanism I).

with a mechanism in which inhibitory CO and the CH_3 donor substrate bind competitively to the same form of the enzyme. The kinetic parameters given in Figure 2 were obtained by direct fitting to the equation for mechanism I in Scheme 3. The data can also be fit, with essentially equivalent precision, to an alternative model (mechanism II) in which substrate CO binds first followed by CH_3. However, such a fit requires a very small value of K_{ia}, on the order of 2 μM, which, as a consequence, yields similar numerical values for all other parameters ($K_m^{CH_3}$, K_m^{CO}, K_i, and V_{max}). Because the second mechanism is a more complex situation that would require unprecedented binding of 2 mol of CO, values are given (Figure 2) only for the best fit to mechanism I. The direct competition of inhibitory CO with the CH_3 donor is nonetheless characteristic and is implicated in either case.

Characterization of the ACDS β Subunit F195A Variant. *Decreased Reactivity with the Corrinoid CH_3 Donor.* Previous crystallographic studies of CODH/ACS suggested that reorientation of a strictly conserved phenylalanine residue Phe 512 (Phe 195 in the ACDS β subunit) provides access of CO from the tunnel to the axial position of Ni_p in the closed form of the enzyme, whereas in the open conformation, axial approach to Ni_p would be shielded by repositioning of the phenyl side chain to lie within the coordination sphere above Ni_p.[2,5] In addition, the large apparent K_m for CO in open-only forms of ACS was previously

dx.doi.org/10.1021/bi3016718 | Biochemistry 2013, 52, 1705−1716

Scheme 3. Steady-State Kinetic Mechanism of Acetyl-CoA Synthase[a]

Mechanism I: CH_3 binds first

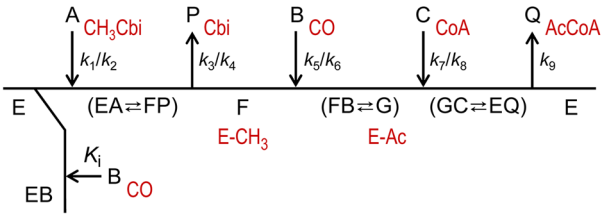

$$\frac{1}{v} = \frac{K_{mA}}{V_{max}}\frac{1}{[A]}\left(1+\frac{[B]}{K_i}\right) + \frac{K_{mB}}{V_{max}}\frac{1}{[B]} + \frac{K_{mC}}{V_{max}}\frac{1}{[C]} + \frac{K_{ib}K_{mC}}{V_{max}}\frac{1}{[B][C]} + \frac{1}{V_{max}}$$

$$\frac{1}{v} = \frac{K_{mA}}{V_{max}}\frac{1}{[A]}\left(1+\frac{[B]}{K_i}\right) + \frac{K_{mB}}{V_{max}}\frac{1}{[B]} + \frac{1}{V_{max}}$$ Simplified form at high [CoA]

Mechanism II: CO binds first

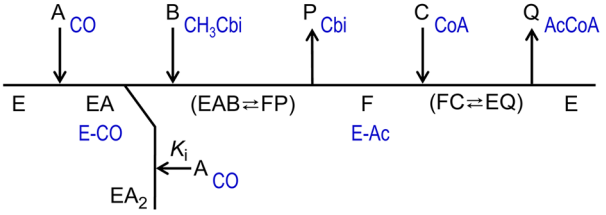

$$\frac{1}{v} = \frac{K_{mB}}{V_{max}}\frac{1}{[B]}\left(1+\frac{[A]}{K_i}\right) + \frac{K_{mA}}{V_{max}}\frac{1}{[A]} + \frac{K_{mC}}{V_{max}}\frac{1}{[C]} + \frac{K_{ia}K_{mB}}{V_{max}}\frac{1}{[A][B]} + \frac{1}{V_{max}}$$

$$\frac{1}{v} = \frac{K_{mB}}{V_{max}}\frac{1}{[B]}\left(1+\frac{[A]}{K_i}+\frac{K_{ia}}{[A]}\right) + \frac{K_{mA}}{V_{max}}\frac{1}{[A]} + \frac{1}{V_{max}}$$ Simplified form at high [CoA]

[a]Two mechanisms consistent with the data are depicted. Simplified rate equations are obtained under conditions in which CoA concentration is much larger than the value of K_m^{CoA} (estimated previously to be ≈20 μM).[15] For mechanism I, the kinetic parameters are defined as

$$K_m^{CH_3} = \frac{k_9(k_2+k_3)}{k_1(k_3+k_9)};\ K_m^{CO} = \frac{k_3k_9}{k_5(k_3+k_9)};\ K_m^{CoA} = \frac{k_3(k_8+k_9)}{k_7(k_3+k_9)};\ k_{cat} = \frac{k_3k_9}{k_3+k_9};\ V_{max} = k_{cat}[E]_{tot}$$

where odd-numbered rate constants correspond to steps running in the overall forward direction of acetyl-CoA synthesis and even-numbered constants denote the reverse. In mechanism I, $K_{ib} = k_6/k_5$, as defined for substrate B (CO). CO substrate binding and dissociation in mechanism II correspond to the equality $K_{ia} = k_2/k_1$ in that mechanism. In the text, V_{max} is expressed as a turnover number, which is equivalent to k_{cat}. Derivations were according to Segel.[43]

interpreted to be due to steric hindrance of CO access to the Ni_p axial position in the open state.[6] Therefore, the ACDS β subunit F195A form was overexpressed in *E. coli*, purified, and characterized to determine what effects this alteration would have on enzyme function and whether evidence could be obtained for a change in the accessibility of CO to Ni_p.

As shown in Figure 3, stopped-flow analysis of the enzyme reaction with methylcobinamide in the absence of other substrates revealed markedly lower reactivity of the F195A

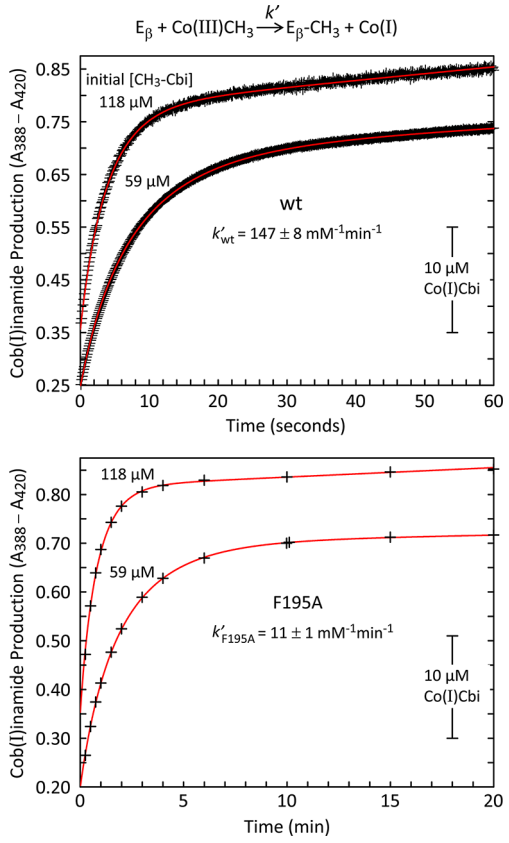

Figure 3. Stopped-flow analysis of the methyl transfer to the ACDS β subunit and comparison with the F195A form. Anaerobic stopped-flow reactions for the wild-type enzyme (wt, top panel) and standard spectrophotometric measurements for the variant (F195A, bottom panel) were performed as described in Materials and Methods at the indicated levels of methylcobinamide present initially after mixing the Ti^{3+}-reduced protein with methylcobinamide. The final protein concentration was 22.6 μM for both enzymes. The solid red lines are drawn from numerical fits of the product absorbance data to a rate equation that contained two terms, a second-order expression for the reaction of the enzyme with CH_3-cobinamide and a first-order component to account for a degree of photolysis of the substrate produced by light emitted from the deuterium lamp of the diode array spectrophotometer. In the bottom panel, the shutter was kept closed between measurements, and the extent of correction was notably reduced. Under the same conditions, the wild-type enzyme showed similarly low levels of photolysis, but methylation was too fast to follow. The extent of methylation was 96–99% for the wild type, as measured separately with manual mixing in a standard cuvette, and approximately 94% for the F195A variant.

form, which proceeded at a rate approximately $^1/_{14}$th of the rate of the wild-type enzyme. Near stoichiometric equivalence was observed for methylation of both enzymes, which stands in contrast to observations with CODH/ACS where only ~50% of the enzyme could be methylated[17,20] and also is unlike the case of recombinant *M. thermoacetica* ACS, which acquired 2.2 methyl groups in the reaction with radiolabeled methylcobinamide.[21] The decreased methyl transfer activity of the F195A variant also resulted in an increase in the $K_m^{CH_3}$ in overall acetyl-CoA synthesis. As shown in Figure 4, the activity of the F195A form continued to increase steadily as the methylcobinamide concentration was increased to the highest level tested (0.8 mM), which indicates an increased value for $K_m^{CH_3}$ and also suggests that V_{max} for the variant may be similar in

dx.doi.org/10.1021/bi3016718 | *Biochemistry* 2013, 52, 1705–1716

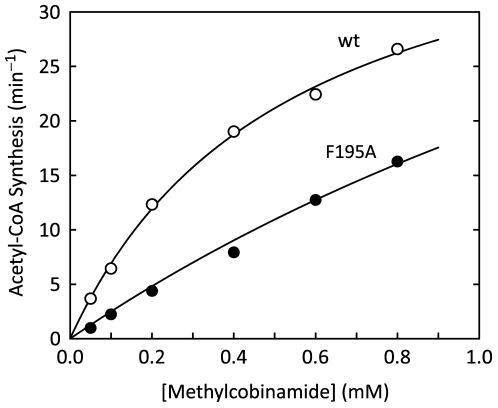

Figure 4. The F195A variant exhibits an increased K_m for methylcobinamide in acetyl-CoA synthesis. Acetyl-CoA synthesis reactions were performed with the F195A enzyme using 6% CO in N_2. For comparison, data are shown at 50% CO for the wild-type enzyme, where K_i is ~5 times greater. The line drawn for the F195A form relies on the apparent V_{max} value at this level of CO calculated from the rate equation for mechanism I in Scheme 3, using the same value for the true V_{max} as the wild type (Figure 2). The fit gives a $K_m^{CH_3}$ of 2.4 mM for the variant that can be compared with the value of 1.9 ± 0.5 mM given in the legend of Figure 1.

magnitude to that of the wild type. Because only a small degree of saturation with the methyl donor could be achieved with the variant enzyme, a full description of the F195A kinetic pattern was limited. However, if V_{max} is similar to the wild type as the data suggest, then a fit of the data in Figure 4 to mechanism I provides an estimate of $K_m^{CH_3}$ that is ~3-fold greater than that of the wild-type enzyme. As defined in Scheme 3, the $K_m^{CH_3}$ is predicted to increase mainly as a result of a decreased value for k_1 and/or k_3.[a] Thus, the observation of an increase in $K_m^{CH_3}$ is consistent with a decreased second-order rate constant for methylation and reflects a significant portion of the effect seen in the stopped-flow experiments.

Increased Reactivity with CO. The acetyl-CoA synthesis activity of the ACDS β subunit F195A form was measured at varying concentrations of dissolved CO, obtained by equilibration of reaction mixtures under different headspace gas compositions of CO in N_2. The results shown in Figure 1 (filled symbols) indicate a marked increase in the reactivity of the F195A form with CO, both as a substrate and as an inhibitor. The K_i value decreased to ~$^1/_5$th of that of the wild type, indicating substantially greater CO substrate inhibition. The K_m^{CO} also declined, indicating a marked increase in reactivity toward CO acting as a substrate, as well. Moreover, the V_{max}/K_m^{CO} ratio [which is equivalent to k_5, i.e., the reaction of CO with the methylated enzyme (Scheme 3)] increases approximately 60-fold, from a value of ~200 mM^{-1} min^{-1} in the wild type to roughly 12000 mM^{-1} min^{-1} in the F195A variant. Thus, the effect on CO acting as a substrate was substantially larger than the 5-fold effect on the K_i. The value of k_5 could be estimated only roughly for the variant, because of uncertainty in the value of K_m^{CO} due to difficulty in obtaining accurate initial rate measurements at very low CO concentrations. Nevertheless, it is notable that the k_{cat}/K_m^{CO} ratio is insensitive to the value of V_{max} chosen to fit the data in Figure 1 and is unaffected throughout the entire range of reasonable values for V_{max}. The consequence of the much greater influence on K_m^{CO} relative to that of K_i is seen in Figure 1, where, at low levels of CO, the activity of the variant enzyme actually exceeds that of the wild type.

EPR Spectroscopic Characterization of Binding of CO to the Wild Type and F195A Variant. In the absence of a methyl donor substrate, CO interacts with ACS to form a paramagnetic Ni$^+$-CO adduct.[6,14,22−29] Two major forms of the EPR signal that differ primarily in their $g_{x,y}$ values have been observed, designated types I ($g_{x,y}$ ~ 2.08−2.09) and II ($g_{x,y}$ ~ 2.05−2.06). In Figure 5, the two Ni$^+$-CO signal types are

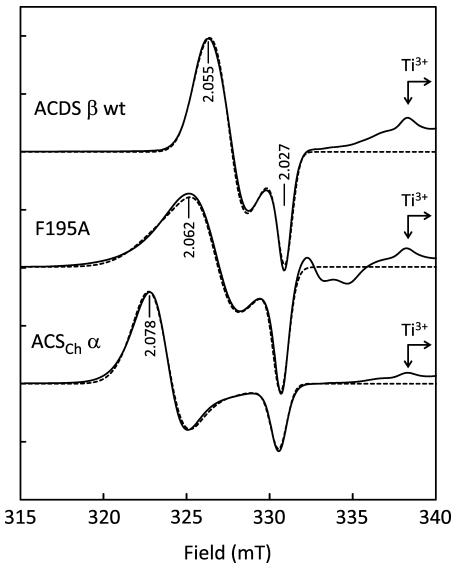

Figure 5. Ni$^+$-CO EPR spectrum of the F195A variant compared with that of the wild-type ACDS β subunit and bacterial ACS from *Carboxydothermus hydrogenoformans*. Representative X-band EPR spectra were obtained following reaction of the proteins with CO in the presence of 0.5 mM Ti citrate as described in Materials and Methods. Simulated spectra shown as dashed lines were obtained using the Biomolecular EPR spectroscopy software package[44] with g_1, g_2, and g_3 and W_1, W_2, and W_3 values of 2.056, 2.046, and 2.026 and 10.0, 9.0, and 5.0, respectively, for wild-type ACDS β; 2.070, 2.053, and 2.028 and 22.0, 12.0, and 5.0, respectively, for F195A; and 2.076, 2.072, and 2.0285 and 15.0, 11.0, and 5.5, respectively, for ACS$_{Ch}$ α. A portion of the signal due to added Ti^{3+} is indicated in the region at the right.

compared with the spectrum of the ACDS β subunit F195A form. The EPR spectrum of the variant was altered such that significant resonance now extends into the lower-field, higher-$g_{x,y}$ = 2.08−2.09 region typical of the type I species. The results confirm that the electronic properties of the A cluster indeed are affected by the presence or absence of the Phe 195 phenyl side chain and are consistent with a potential direct influence of that group on the coordination environment and reactivity of Ni_p.

Recent findings indicate that EPR signal types I and II report on the conformational states of the enzyme;[6] type I is observed in enzyme systems capable of adopting the closed form, in which interdomain (ACS) or intersubunit (ACDS) contacts are present, and type II is characteristic of systems that assume the open conformation, such as the isolated ACDS β and the N-terminally truncated bacterial enzyme ACS$_{Ch}$ΔN. Previous studies also indicate that the maximal intensity of the type I signal is produced at very low CO concentrations;[30−32] however, little or no data have been published on the CO concentration dependence of open-form signal type II.

dx.doi.org/10.1021/bi3016718 | *Biochemistry* 2013, 52, 1705−1716

Therefore, titrations of the ACDS β subunit with CO were conducted by incubation of enzyme samples with different gas mixtures of CO in N_2 in the presence of Ti citrate as a reducing agent. As described in Materials and Methods, CO partial pressures in excess of 1 atm were produced and held until the reaction mixtures had been frozen by use of an apparatus that permits effective gas equilibration, incubation, and subsequent transfer of the samples to the EPR tube, all while maintaining a controlled positive pressure in the system. The results (Figure 6) show that unlike acetyl-CoA synthesis activity, the Ni^+-CO

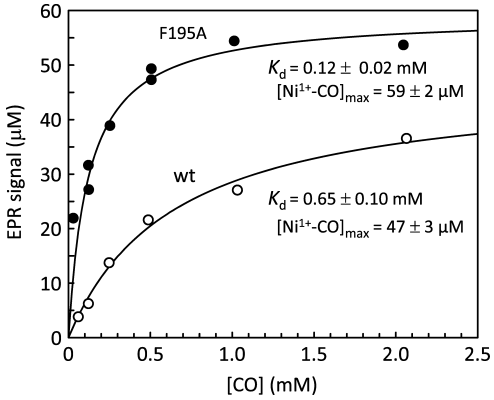

Figure 6. CO titration of the Ti citrate-reduced wild-type ACDS β subunit and F195A variant measured by EPR. Mixtures containing 105 μM wild-type or 104 μM F195A protein in the presence of 0.5 mM Ti citrate were equilibrated with CO/N_2 gas mixtures to provide the indicated final dissolved CO concentrations. The reaction conditions and apparatus needed to maintain partial pressures of CO higher than 1 atm until after freezing and the conditions for EPR spectroscopy and spin quantification are described in Materials and Methods. Lines of best fit are drawn according to the binding isotherm $[Ni^+\text{-}CO] = [Ni^+\text{-}CO]_{max}[CO]/(K_d + [CO])$, which applies under conditions where the dissolved CO concentration is kept constant in equilibrium with the gas phase.

spin concentration does not decline at high CO concentrations but instead follows a hyperbolic saturation curve, with apparent K_d values of 0.65 ± 0.10 and 0.12 ± 0.02 mM for the wild-type ACDS β subunit and F195A form, respectively. The saturation behavior of wild-type and variant enzymes closely paralleled the kinetically determined K_i values for CO substrate inhibition. The results provide additional confirmation that CO reactivity is increased in the F195A variant and also show that formation of the Ni^+-CO species is closely correlated with the production of an inhibited form of the enzyme.

DISCUSSION

Acetyl-CoA synthesis by ACS is a three-substrate, two-product reaction that uses the substrates CoA, CO, and methyl-Co(III)corrinoid and generates acetyl-CoA and Co(I)corrinoid as products. The enzyme active site contains a metal center, the A cluster, that encompasses two Ni atoms and an $[Fe_4S_4]$ center.[2,3,33,34] Distinct open and closed conformational states have been described for bacterial ACS.[2,5] In the open state, the A cluster is more accessible to large substrates such as CoA and CH_3-corrinoid, because of a decreased extent of contact of the N-terminal domain with the central and C-terminal regions. In the closed form, the A cluster is buried such that CO is the only substrate capable of reaching the A cluster, and then only by means of the tunnel that extends through the N-terminal domain and ends at Ni_p. As shown in Scheme 2, the strictly conserved Phe 512 residue (Phe 195 in the ACDS β subunit) that blocks axial approach to Ni_p in the open form is repositioned away from Ni_p in the closed form such that CO access from the tunnel becomes unobstructed.

CO Inhibits Open and Closed Conformational Forms of ACS. Earlier results suggested the existence of different modes of interaction of CO with the A cluster during acetyl-CoA synthesis, with CO acting both as a substrate and an inhibitor of acetyl-CoA formation in reactions with CODH/ACS as well as with the isolated full-length ACS subunit.[6,16] The kinetics of interactions of CO with bacterial ACS (from *C. hydrogenoformans*, ACS_{Ch}) are markedly altered by truncation of the N-terminal domain.[6] A low value of <10 μM was estimated for the apparent K_m^{CO} of the full-length enzyme, which increased to 0.36 mM in the $ACS_{Ch}\Delta N$ protein. In addition, the level of CO inhibition was substantially decreased in the truncated enzyme.

Both $ACS_{Ch}\Delta N$ and the isolated ACDS β subunit proteins represent an "open-like" conformational state because of the inability to engage in protein−protein contacts needed to adopt the closed form. Both enzymes exhibit much higher K_m^{CO} values than the full-length ACS_{Ch}, and both show substantially weaker effects of CO inhibition, to the extent that it was unclear from previous studies whether CO actually inhibits at all the open form enzymes.[6] In this study, the steady-state kinetic pattern provides unequivocal evidence that CO also inhibits acetyl-CoA synthesis by the openlike ACDS β subunit. Thus, the open form is characterized by a lower reactivity toward CO in general, with K_m^{CO} and K_i values (Figure 1) that are both substantially higher than in the closed form. The results are consistent with the hypothesis that CO inhibition is a characteristic intrinsic to catalysis at the A cluster.[b]

Inhibitory CO Competes with CH_3. Because the ACS kinetic pattern in which both CO and CH_3 donor substrates are varied had not been determined previously, the effects of CO inhibition in the context of the overall kinetic mechanism remained to be established. The steady-state pattern for synthesis of acetyl-CoA by the ACDS β subunit (Figure 2 and Scheme 3) was found to fit two possible kinetic mechanisms. Both models indicate that inhibitory CO and the CH_3-corrinoid substrate compete for a common form of the enzyme. Studies on CODH/ACS from *M. thermoacetica* by Tan et al.[17] demonstrated CO inhibition of the partial reaction of the methyl group transfer from the methylcorrinoid protein to ACS. A subsequent kinetic model, developed purely on the basis of the effects of CO and CoA on the methylation−demethylation reaction of CODH/ACS with CH_3-corrinoid protein, included a CO-inhibited species produced by competition of CO with the CH_3 donor for the same state of the enzyme.[20] Our results agree with that indication and demonstrate in addition that inhibition during turnover in acetyl-CoA synthesis is similarly due to direct competition of CO with the methyl substrate for the same form of the enzyme.

The open conformation ACDS β subunit system is well-suited for kinetic analyses of CO interactions at the A cluster. Earlier studies from the Lindahl laboratory described complex behavior of CO binding and kinetics of acetyl-CoA synthesis using the CODH/ACS enzyme.[16,32] In that system, CO interacts at two sites, the A cluster of ACS and the C cluster of CODH, the two sites exhibit coupling, which may be complete or only partial depending on the enzyme preparation, and different conformational states can be adopted, as well. Carbon

dx.doi.org/10.1021/bi3016718 | *Biochemistry* 2013, 52, 1705−1716

monoxide was found to act as an uncompetitive inhibitor with respect to CO_2; however, variation of the CH_3 donor substrate was not employed, and it was not until later[17,20] that CO inhibition by reaction at the A cluster was implicated. In contrast, CO competition with CH_3 for reaction at the A cluster is readily apparent in the less complex kinetics of the open form ACDS β subunit found here. The apparent cooperativity of CO inhibition postulated for CODH/ACS[16,20] does not complicate the kinetics of the ACDS β subunit in which binding of a single inhibitory CO is sufficient to fit the data.

Mechanism of CO Inhibition and Order of Substrate Binding. Carbon monoxide-based deactivation of the nucleophilic reaction of low-valent Ni with an electrophilic CH_3 donor has been considered previously as a consequence of decreased electron density on Ni due to π back-bonding, i.e., electron donation from the reduced metal to the unoccupied π^* structure in CO.[35−37] Thus, a likely basis for inhibition by CO is that competition of CO with CH_3 for a reduced state of the A cluster results in the loss of nucleophilicity of Ni_p. The formation of a weakly nucleophilic Ni_p-CO species that either would be totally incapable of displacing CH_3 from the corrinoid donor or would react very slowly relative to addition of CO to CH_3-Ni_p, therefore, manifests as inhibition by CO.

Both reaction mechanisms in Scheme 3 fit the data essentially equally well, and both indicate that in the absence of a CH_3 donor, CO will interact to generate the inhibited form of the enzyme. The possibility that CO binds before CH_3 (mechanism II) derives support from the finding of substantial amounts of ^{14}C-labeled acetyl-CoA formed in pulse−chase experiments in which ^{14}CO was reacted with ACS_{Ch} in the absence of other substrates followed by dilution into mixtures containing CoA and CH_3-corrinoid and unlabeled CO.[38] Our data indicate that if mechanism II does operate, then it would require a very low value for K_{ia} (binding of CO to the free enzyme) on the order of ~2 μM. From an experimental standpoint, the small value of K_{ia} indicates that it would be essentially impossible to distinguish between mechanisms I and II by additional steady-state measurements, because even at very low levels of CO the kinetic patterns would be nearly identical.

In both models, inhibitory CO must first dissociate before CH_3 can react. Thus, mechanism II could allow for a slow single turnover of ^{14}CO initially associated with ACS to account for the labeled acetyl-CoA formed in the pulse−chase experiments (slow, because the initial rates of [^{14}C]acetyl-CoA synthesis in the chase mixtures containing unlabeled CO were less than 1 min^{-1} according to the data in Table 3 of ref 38). However, the finding that inhibitory CO competes with the CH_3 donor substrate requires that the inhibited enzyme in mechanism II must have bound 2 mol of CO. Although there is no theoretical objection for binding more than one CO to the A cluster, the binding of multiple CO molecules was specifically discounted in FTIR studies where it was concluded that a sole metal-carbonyl species was formed[29,39] at a partial pressure of CO (1 atm) sufficient to produce large amounts of the inhibited form of the enzyme.[c] Thus, the evidence favors the less complex mechanism I, with the possibility remaining (but inconsistently supported) that a low rate of reaction might take place also by mechanism II.

Rate-Limiting Step in Vitro. Stopped-flow measurements yielded a value for the second-order rate constant for methylation of the ACDS β subunit [k' = 147 ± 8 mM^{-1} min^{-1} (Figure 3)] that agrees reasonably well with the $k_{cat}/K_m^{CH_3}$ value of 124 ± 33 mM^{-1} min^{-1} obtained from the steady-state kinetics. Our data indicate that the reaction of CO with the methylated A cluster, i.e., CO insertion, proceeds with a second-order rate constant of ~200 mM^{-1} min^{-1}, which corresponds to the value of k_5 in Scheme 3 given by the k_{cat}/K_m^{CO} ratio. In the variant lacking Phe 195, that value is even higher. The results indicate that in the context of the in vitro behavior of the enzyme, methylation is the most critical reaction that limits catalysis overall. Depending on the prevailing concentrations of CO or CH_3 donor, either methylation, CO insertion, or both can impose a limit on the overall flux of acetyl-CoA formation. However, at moderate levels of CO, the rate of methylation is further restricted by the fraction of free enzyme that exists in the uninhibited state given by $K_i/([CO] + K_i)$. In the wild-type β subunit, a level of CO of ~0.80−0.92 mM would be required to decrease the flux through the methyl transfer step by half, whereas only 0.17 mM CO would suffice to produce the same effect on the F195A form. Thus, in addition to the absolute rate of reaction, under a wide range of experimental conditions, the observed flux is likewise limited by the efficiency of methyl group transfer.

Role of Conserved Phenylalanine in the Coordination Sphere of Ni_p. Substantial changes in the kinetics of acetyl-CoA synthesis were evident in reactions with the ACDS subunit F195A form. Inhibition by CO was significantly more pronounced, with a decrease in the value of K_i that indicates an approximately 5-fold greater sensitivity to CO inhibition relative to that of the wild type. The effect on k_5, the step in which CO reacts as a substrate (Scheme 3), showed that CO substrate reactivity was increased to an even greater extent. The enhanced CO substrate reactivity relative to inhibition explains why at low levels of CO, with an equivalent concentration of CH_3 donor, the activity of the variant enzyme actually exceeds that of the wild type (Figure 1). The CO concentration dependence of the enzyme lacking the Phe 195 side chain is reminiscent of the strong CO inhibition of acetyl-CoA synthesis seen in full-length ACS_{Ch}[6] in which the corresponding Phe residue would be displaced in the closed form to allow unobstructed access of CO to Ni_p via the tunnel. Increased affinity for CO in the F195A form is also indicated by the results of CO titrations monitored by EPR (Figure 6). Thus, the results provide the first functional evidence that the phenyl side chain indeed acts to limit the access of CO to Ni_p.

In contrast to the increased reactivity of the F195A variant with CO, the marked decrease in k' in stopped-flow methylation experiments (Figure 3) and the increase in $K_m^{CH_3}$ in acetyl-CoA synthesis kinetics (Figure 4) show that reactivity with the corrinoid CH_3 donor is substantially diminished. One possible explanation for the decreased methylation activity would involve the loss of the ability to sterically exclude additional ligands from the coordination environment of Ni_p. In the absence of the shielding phenyl group, additional stabilization of the Ni^{2+} oxidation state would be expected by engaging additional polar ligands, e.g., solvent water molecules. Such stabilization would further disfavor the already difficult task of reducing Ni^{2+} to a sufficiently low redox state so that nucleophilic attack on the corrinoid CH_3 group could transpire. In fact, preliminary data from UV−visible measurements on reactions of Ti citrate with the wild-type and F195A proteins (not shown) do suggest a lower rate of reduction of the F195A form.

The results indicate a unique role of Phe 195 acting as a coordination site placeholder. When the phenyl group occupies

Scheme 4. Different Modes of Interaction of CO with Acetyl-CoA Synthase Determined by the Conformational State of the Protein, the Position of Conserved Phe 195 in the Coordination Sphere of Ni_p, and the Presence or Absence of the Methyl Donor Substrate[a]

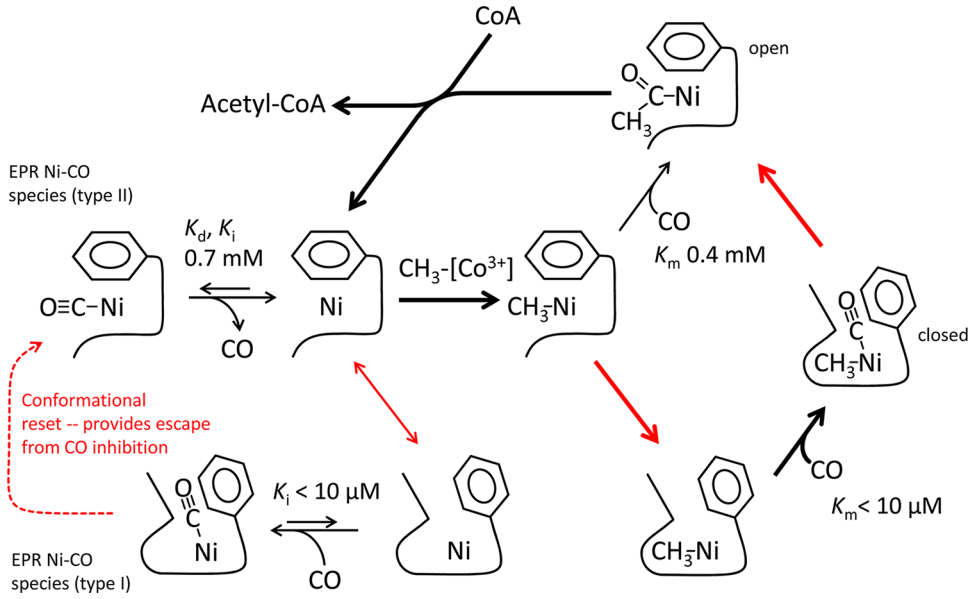

[a]The open conformational state is depicted in the absence of intersubunit or interdomain contacts to the A cluster and with the conserved Phe side chain lying within the coordination sphere of Ni_p and shielding axial approach. The closed conformation is illustrated as a pocketlike arrangement in which the A cluster is buried as a result of protein−protein interactions (e.g., contact with the N-terminal domain in bacterial ACS) in which displacement of the phenyl group permits access of CO solely by means of the tunnel. Red arrows designate changes in conformation; thick arrows trace the catalytic cycle relevant to in vivo conditions with little or no CO freely available in the cytoplasm.

a position in the coordination sphere of Ni it supports the nucleophilic reaction with the methyl donor and impedes reaction with CO, and, when displaced, it sterically unmasks the formed Ni-CH_3 species to increase its reactivity with CO. The implication is that Nature has optimized the catalytic properties of the A cluster by linking conformational changes of the protein to a repositionable aromatic shield that is capable of electronically modulating the reactivity of Ni and sterically governing the most productive order of interaction with substrates.

Relevance of the Ni^+-CO Species to Acetyl-CoA Synthesis. Reaction of CO at the A cluster in the presence of an electron donor produces a paramagnetic Ni^+-CO species that has been a focus in many of the studies on ACS enzymes. Studies from the Ragsdale group demonstrate that the Ni^+-CO species is formed and decays at rates equal to or greater than the rate of overall appearance and disappearance of acetyl-CoA in acetyl-CoA synthesis reactions, and the term "catalytic competence" has been used to describe such kinetic capability.[14,29,39,40] However, because kinetic results generally can be applied only for exclusion of chemical hypotheses, catalytic competence cannot be viewed as evidence that the Ni^+-CO species is an intermediate in catalysis.

Mechanisms that model the Ni^+-CO species as an intermediate can be excluded if they do not fit the data. Behavior consistent with an intermediate requires that the EPR signal must correlate in some unified way with acetyl-CoA synthesis activity. In the closed form enzymes CODH/ACS and ACS, the EPR signal develops at very low CO concentrations but remains undiminished at higher levels where acetyl-CoA synthesis activity undergoes a marked decline, i.e., above 0.02 and 0.1 mM CO for ACS_{Ch}[6] and CODH/ACS,[16] respectively. The results here provide good quantification of similar behavior at substantially higher levels of CO in the open form ACDS β subunit and the F195A form. Neither the wild-type nor the F195A enzyme activity curves (Figure 1) follow the formation of the EPR signal (Figure 6). Instead, the K_d values found in the EPR titrations match well with K_i values determined from the kinetic experiments. The relative changes in K_i and K_d for the variant and the wild type are likewise very similar. In contrast, formation of the Ni^+-CO species does not correlate with the K_m or the changes in K_m for CO acting as substrate, as would be expected if that species were produced as an intermediate. None of the mechanistic schemes proposed so far that place the Ni^+-CO species as an intermediate are consistent with these results, and such mechanisms must therefore be excluded. Rather, if the Ni^+-CO species is modeled as an inhibited form of the enzyme, then relatively uncomplicated solutions (Scheme 3) are found that fit the data.

The conclusion is that the Ni^+-CO species is a nonproductive, dead-end inhibitor in equilibrium with the free form of the enzyme that reacts with CH_3. The reason that the inhibited state can appear to be kinetically viable or "catalytically competent" but not be an intermediate in catalysis is because production of acetyl-CoA will resume at the maximal rate possible immediately upon re-entry of uninhibited enzyme back into the catalytic cycle. The inhibited state is likewise quickly re-formed as soon as the methyl donor substrate is exhausted and acetyl-CoA synthesis halts. And, similarly, EPR signal rapidly reappears in the presence of CO after addition of CoA to the isolated acetyl-bound enzyme,[21] which regenerates the uncombined state of the enzyme to react with CO. Those results do not conflict with our here, but at the same time, the observed kinetic pattern cannot be reconciled with the Ni^+-CO species as an intermediate.

dx.doi.org/10.1021/bi3016718 | Biochemistry 2013, 52, 1705−1716

Conformational Control of Catalysis at the A Cluster and Escape from CO Inhibition in Vivo. Inhibition by CO is encountered in many metalloprotein systems ranging from hemoglobin to hydrogenases. Because our results indicate that CO inhibition may be an intrinsic characteristic of catalysis at the A cluster Ni−Fe center, it is reasonable to ask what methods Nature has found to minimize or circumvent such effects in the enzyme. All the more challenging is the situation in which CO is also required as a substrate for the reaction. A working model that involves CO compartmentalization (gas channel) and conformational changes linked to repositioning of the conserved Phe residue is presented in Scheme 4. Multiple modes of CO binding are depicted, with CO acting as both substrate and an inhibitor, with low affinity (open conformation) or high affinity (closed state). In contrast to CO, interaction with methylcorrinoid can take place only with the open conformation because the A cluster is buried and inaccessible to large substrates in the closed form. Accordingly, the central reaction in the scheme is the conversion of the open form enzyme to an open-state methylated species. At high levels of CO, such as those available under in vitro assay conditions, facile formation of an enzyme-acetyl species can take place (thin black arrow up), which when captured by CoA leads to high turnover rates of acetyl-CoA synthesis. Under certain chemolithoautotrophic growth conditions where CO is abundant, conditions that also could have existed for a primordial A cluster protein, this "open-only" pathway may be quite significant. However, at low concentrations of CO in the cytoplasm, an alternative pathway is needed to increase reactivity with CO. Production of CO from CO_2 by CODH and containment in the tunnel clearly would be one way to increase the reaction rate, which also acts to flatten the overall thermodynamic landscape for the reaction.[41] In addition, as evidenced by the properties of the F195A variant, displacement of the phenyl side chain by itself contributes markedly to decrease the K_m for CO and increase CO reactivity at Ni_p. Thus, a conformational change coupled to the steric unmasking of the Ni-CH_3 species (thick red arrow down) could allow for the subsequent arrival of CO to support formation of an Ni(CO)CH_3 intermediate.

On the basis of [1-^{14}C]acetyl-CoA/CO carbonyl exchange studies of ACDS and full-length and truncated ACS_{Ch}, it was previously indicated that ACS must be able to adopt the closed state to promote the formation of a fragmented Ni(CO)CH_3 intermediate, and that following acetyl C−C bond formation, the Ni-acetyl species is relatively much more stable in the open form.[6] Reaction of the ACDS β subunit open form Ni-acetyl species is known to proceed at a very high rate of ∼10800 min^{-1}, and therefore upon return to the open form, access of the Ni-acetyl species to CoA rapidly generates a molecule of acetyl-CoA.

The effect that CO containment has to enhance substrate reactivity likewise causes an unwanted increase in CO inhibition. The implication of a binding pocket for CO adjacent to Ni_p in the closed form CODH/ACS structure[42] was considered to explain the very rapid recombination of CO after photolysis[29] and thus likely contributes to the increased affinity of CO in the closed conformation. However, even in the open form, inhibition also becomes significantly greater when access to Ni_p is increased by removal of the shielding phenyl group, as indicated by the lower K_i and K_d values for CO in the ACDS β subunit F195A form. Thus, if remethylation of Ni is not achieved after acetyl-CoA dissociates during the time that the enzyme exists in the open form, then a conformational change to the closed form (thin red double-headed arrow) would convert the enzyme into a state that is highly susceptible to inhibition. Arrival of CO at the A cluster in the absence of CH_3 would then generate the inhibited form of the enzyme containing tightly bound CO detectable by EPR as the Ni^+-CO type I signal. Dissociation of CO from this state is most unfavorable, and simple reversal of the reaction is least likely, as indicated by the low K_i value of <10 μM for ACS_{Ch},[6] and by the very low levels of CO needed to produce maximal EPR signal formation with CODH/ACS, with a K_d estimated to be ∼3 μM.[31] To recover from this dead-end complex, a "conformational reset" to the open state (dashed red line), in which the K_d and K_i for CO dissociation are much higher, could allow for escape of CO and return of the enzyme to the catalytic cycle, a process that would be favored additionally by the low CO concentration in vivo. Whether interaction with the corrinoid protein might trigger the conformational change or impart energy needed to convert to the open state is an interesting possibility that remains to be investigated.

In summary, it appears that Nature selected the aromatic phenyl moiety to modulate the reactivity of Ni in concert with protein conformational changes to increase the efficiency of acetyl-CoA synthesis. The hydrophobic nature of this group acts to enhance the reactivity of Ni with CH_3 in the open state, in which the Phe residue also provides steric interference that mitigates inhibition by CO. The ability of the rigid phenyl side chain to retreat as the conformation closes and CO enters from the channel then exposes the CH_3-Ni species in a state with maximal reactivity to undergo carbonylation. The enzyme thereby acquired the means to handle special requirements of organometallic chemistry, to capitalize on the most productive reaction sequence and avoid intrinsic CO inhibition.

■ AUTHOR INFORMATION

Corresponding Author

*Department of Biochemistry and Molecular Biology, Uniformed Services University of the Health Sciences, 4301 Jones Bridge Rd., Bethesda, MD 20814. Telephone: (301) 295-3555. Fax: (301) 295-3512. E-mail: david.grahame@usuhs.edu.

Present Address

‖College of Sciences, Georgia Institute of Technology, 225 North Ave., Atlanta, GA 30332.

Funding

This work was supported by National Science Foundation Grant MCB-0923766 and Uniformed Services University of the Health Sciences Grant R071IX (D.A.G.) and by National Science Foundation Grant CHE-0848196 (E.C.D.).

Notes

The authors declare no competing financial interest.

■ ABBREVIATIONS

ACDS, five-subunit acetyl-CoA decarbonylase/synthase complex in Archaea; ACS, acetyl-CoA synthase; ACS_{Ch}, ACS from *Carboxydothermus hydrogenoformans*; ACS_{Mt}, ACS from *Moorella thermoacetica*; CODH, carbon monoxide dehydrogenase; CODH/ACS, bifunctional CO dehydrogenase/acetyl-CoA synthase $\alpha_2\beta_2$ enzyme; EPR, electron paramagnetic resonance; FTIR, Fourier transform infrared spectroscopy; Ni_p, Ni atom in the A cluster proximal to the [Fe_4S_4] component.

■ ADDITIONAL NOTES

[a]The relative effect on $K_m^{CH_3}$ under conditions where k_{cat} is unchanged is given by the ratio of $K_m^{CH_3}/k_{cat} = (k_2 + k_3)/k_1k_3$, so that the degree of variation in $K_m^{CH_3}$ also may be influenced by the magnitude of k_2.

[b]This is not contradicted by the fact that CO inhibition is weaker in the open form, because the decreased inhibitory effect is also accompanied by substantially lower CO substrate reactivity.

[c]Unpublished experiments by K. A. Bagley and D. A. Grahame also reveal only a single major metal-carbonyl resonance by FTIR using either ACS_{Ch} or the ACDS β subunit.

■ REFERENCES

(1) Doukov, T. I., Iverson, T. M., Seravalli, J., Ragsdale, S. W., and Drennan, C. L. (2002) A Ni-Fe-Cu center in a bifunctional carbon monoxide dehydrogenase/acetyl-CoA synthase. *Science 298*, 567−572.

(2) Darnault, C., Volbeda, A., Kim, E. J., Legrand, P., Vernede, X., Lindahl, P. A., and Fontecilla-Camps, J. C. (2003) Ni-Zn-[Fe_4-S_4] and Ni-Ni-[Fe_4-S_4] clusters in closed and open subunits of acetyl-CoA synthase/carbon monoxide dehydrogenase. *Nat. Struct. Biol. 10*, 271−279.

(3) Svetlitchnyi, V., Dobbek, H., Meyer-Klaucke, W., Meins, T., Thiele, B., Romer, P., Huber, R., and Meyer, O. (2004) A functional Ni-Ni-[4Fe-4S] cluster in the monomeric acetyl-CoA synthase from *Carboxydothermus hydrogenoformans*. *Proc. Natl. Acad. Sci. U.S.A. 101*, 446−451.

(4) Marchler-Bauer, A., Lu, S., Anderson, J. B., Chitsaz, F., Derbyshire, M. K., DeWeese-Scott, C., Fong, J. H., Geer, L. Y., Geer, R. C., Gonzales, N. R., Gwadz, M., Hurwitz, D. I., Jackson, J. D., Ke, Z., Lanczycki, C. J., Lu, F., Marchler, G. H., Mullokandov, M., Omelchenko, M. V., Robertson, C. L., Song, J. S., Thanki, N., Yamashita, R. A., Zhang, D., Zhang, N., Zheng, C., and Bryant, S. H. (2011) CDD: A Conserved Domain Database for the functional annotation of proteins. *Nucleic Acids Res. 39*, D225−D229.

(5) Volbeda, A., and Fontecilla-Camps, J. C. (2004) Crystallographic evidence for a CO/CO_2 tunnel gating mechanism in the bifunctional carbon monoxide dehydrogenase/acetyl coenzyme A synthase from *Moorella thermoacetica*. *J. Biol. Inorg. Chem. 9*, 525−532.

(6) Gencic, S., Duin, E. C., and Grahame, D. A. (2010) Tight coupling of partial reactions in the acetyl-CoA decarbonylase/synthase (ACDS) multienzyme complex from *Methanosarcina thermophila*: Acetyl C-C bond fragmentation at the A cluster promoted by protein conformational changes. *J. Biol. Chem. 285*, 15450−15463.

(7) Zou, X., Evans, D. R., and Brown, K. L. (1995) Efficient and convenient method for axial nucleotide removal from vitamin B12 and its derivatives. *Inorg. Chem. 34*, 1634−1635.

(8) Gencic, S., and Grahame, D. A. (2008) Two separate one-electron steps in the reductive activation of the A cluster in subunit β of the ACDS complex in *Methanosarcina thermophila*. *Biochemistry 47*, 5544−5555.

(9) Gencic, S., and Grahame, D. A. (2003) Nickel in subunit β of the acetyl-CoA decarbonylase/synthase multienzyme complex in methanogens. Catalytic properties and evidence for a binuclear Ni-Ni site. *J. Biol. Chem. 278*, 6101−6110.

(10) Grahame, D. A. (2011) Methods for analysis of acetyl-CoA synthase: Applications to bacterial and archaeal systems. *Methods Enzymol. 494*, 189−217.

(11) Tonomura, B., Nakatani, H., Ohnishi, M., Yamaguchi-Ito, J., and Hiromi, K. (1978) Test reactions for a stopped-flow apparatus. Reduction of 2,6-dichlorophenolindophenol and potassium ferricyanide by L-ascorbic acid. *Anal. Biochem. 84*, 370−383.

(12) Dean, J. A. (1992) *Lange's Handbook of Chemistry*, 14th ed., McGraw-Hill, Inc., New York.

(13) Lu, W. P., and Ragsdale, S. W. (1991) Reductive activation of the coenzyme A/acetyl-CoA isotopic exchange reaction catalyzed by carbon monoxide dehydrogenase from *Clostridium thermoaceticum* and its inhibition by nitrous oxide and carbon monoxide. *J. Biol. Chem. 266*, 3554−3564.

(14) Seravalli, J., Kumar, M., and Ragsdale, S. W. (2002) Rapid kinetic studies of acetyl-CoA synthesis: Evidence supporting the catalytic intermediacy of a paramagnetic NiFeC species in the autotrophic Wood-Ljungdahl pathway. *Biochemistry 41*, 1807−1819.

(15) Bhaskar, B., DeMoll, E., and Grahame, D. A. (1998) Redox-dependent acetyl transfer partial reaction of the acetyl-CoA decarbonylase/synthase complex: Kinetics and mechanism. *Biochemistry 37*, 14491−14499.

(16) Maynard, E. L., Sewell, C., and Lindahl, P. A. (2001) Kinetic mechanism of acetyl-CoA synthase: Steady-state synthesis at variable CO/CO_2 pressures. *J. Am. Chem. Soc. 123*, 4697−4703.

(17) Tan, X. S., Sewell, C., and Lindahl, P. A. (2002) Stopped-flow kinetics of methyl group transfer between the corrinoid-iron-sulfur protein and acetyl-coenzyme A synthase from *Clostridium thermoaceticum*. *J. Am. Chem. Soc. 124*, 6277−6284.

(18) Tan, X., Sewell, C., Yang, Q., and Lindahl, P. A. (2003) Reduction and methyl transfer kinetics of the α subunit from acetyl coenzyme A synthase. *J. Am. Chem. Soc. 125*, 318−319.

(19) Tan, X., Loke, H. K., Fitch, S., and Lindahl, P. A. (2005) The tunnel of acetyl-coenzyme A synthase/carbon monoxide dehydrogenase regulates delivery of CO to the active site. *J. Am. Chem. Soc. 127*, 5833−5839.

(20) Tan, X., Surovtsev, I. V., and Lindahl, P. A. (2006) Kinetics of CO insertion and acetyl group transfer steps, and a model of the acetyl-CoA synthase catalytic mechanism. *J. Am. Chem. Soc. 128*, 12331−12338.

(21) Bender, G., and Ragsdale, S. W. (2011) Evidence that ferredoxin interfaces with an internal redox shuttle in acetyl-CoA synthase during reductive activation and catalysis. *Biochemistry 50*, 276−286.

(22) Ragsdale, S. W., Ljungdahl, L. G., and DerVartanian, D. V. (1982) EPR evidence for nickel-substrate interaction in carbon monoxide dehydrogenase from *Clostridium thermoaceticum*. *Biochem. Biophys. Res. Commun. 108*, 658−663.

(23) Ragsdale, S. W., Ljungdahl, L. G., and DerVartanian, D. V. (1983) ^{13}C and ^{61}Ni isotope substitutions confirm the presence of a nickel (III)-carbon species in acetogenic CO dehydrogenases. *Biochem. Biophys. Res. Commun. 115*, 658−665.

(24) Ragsdale, S. W., Wood, H. G., and Antholine, W. E. (1985) Evidence that an iron-nickel-carbon complex is formed by reaction of CO with the CO dehydrogenase from *Clostridium thermoaceticum*. *Proc. Natl. Acad. Sci. U.S.A. 82*, 6811−6814.

(25) Lindahl, P. A., Munck, E., and Ragsdale, S. W. (1990) CO dehydrogenase from *Clostridium thermoaceticum*. EPR and electrochemical studies in CO_2 and argon atmospheres. *J. Biol. Chem. 265*, 3873−3879.

(26) Grahame, D. A., Khangulov, S., and DeMoll, E. (1996) Reactivity of a paramagnetic enzyme-CO adduct in acetyl-CoA synthesis and cleavage. *Biochemistry 35*, 593−600.

(27) Terlesky, K. C., Barber, M. J., Aceti, D. J., and Ferry, J. G. (1987) EPR properties of the Ni-Fe-C center in an enzyme complex with carbon monoxide dehydrogenase activity from acetate-grown *Methanosarcina thermophila*. Evidence that acetyl-CoA is a physiological substrate. *J. Biol. Chem. 262*, 15392−15395.

(28) Barondeau, D. P., and Lindahl, P. A. (1997) Methylation of carbon monoxide dehydrogenase from *Clostridium thermoaceticum* and mechanism of acetyl coenzyme A synthesis. *J. Am. Chem. Soc. 119*, 3959−3970.

(29) Bender, G., Stich, T. A., Yan, L., Britt, R. D., Cramer, S. P., and Ragsdale, S. W. (2010) Infrared and EPR spectroscopic characterization of a Ni(I) species formed by photolysis of a catalytically competent Ni(I)-CO intermediate in the acetyl-CoA synthase reaction. *Biochemistry 49*, 7516−7523.

(30) Shin, W., Stafford, P. R., and Lindahl, P. A. (1992) Redox titrations of carbon monoxide dehydrogenase from *Clostridium thermoaceticum*. *Biochemistry 31*, 6003−6011.

(31) Russell, W. K., and Lindahl, P. A. (1998) CO/CO_2 potentiometric titrations of carbon monoxide dehydrogenase from

Clostridium thermoaceticum and the effect of CO_2. *Biochemistry 37*, 10016−10026.
(32) Fraser, D. M., and Lindahl, P. A. (1999) Stoichiometric CO reductive titrations of acetyl-CoA synthase (carbon monoxide dehydrogenase) from *Clostridium thermoaceticum*. *Biochemistry 38*, 15697−15705.
(33) Bender, G., Pierce, E., Hill, J. A., Darty, J. E., and Ragsdale, S. W. (2011) Metal centers in the anaerobic microbial metabolism of CO and CO_2. *Metallomics 3*, 797−815.
(34) Fontecilla-Camps, J. C., Amara, P., Cavazza, C., Nicolet, Y., and Volbeda, A. (2009) Structure-function relationships of anaerobic gas-processing metalloenzymes. *Nature 460*, 814−822.
(35) Lindahl, P. A. (2004) Acetyl-coenzyme A synthase: The case for a $Ni_p(0)$-based mechanism of catalysis. *J. Biol. Inorg. Chem. 9*, 516−524.
(36) Eckert, N. A., Dougherty, W. G., Yap, G. P. A., and Riordan, C. G. (2007) Methyl transfer from methylcobaloxime to (triphos)Ni-(PPh_3): Relevance to the mechanism of acetyl coenzyme A synthase. *J. Am. Chem. Soc. 129*, 9286−9287.
(37) Ito, M., Kotera, M., Matsumoto, T., and Tatsumi, K. (2009) Dinuclear nickel complexes modeling the structure and function of the acetyl CoA synthase active site. *Proc. Natl. Acad. Sci. U.S.A. 106*, 11862−11866.
(38) Seravalli, J., and Ragsdale, S. W. (2008) Pulse-chase studies of the synthesis of acetyl-CoA by carbon monoxide dehydrogenase/acetyl-CoA synthase: Evidence for a random mechanism of methyl and carbonyl addition. *J. Biol. Chem. 283*, 8384−8394.
(39) George, S. J., Seravalli, J., and Ragsdale, S. W. (2005) EPR and infrared spectroscopic evidence that a kinetically competent paramagnetic intermediate is formed when acetyl-coenzyme A synthase reacts with CO. *J. Am. Chem. Soc. 127*, 13500−13501.
(40) Gorst, C. M., and Ragsdale, S. W. (1991) Characterization of the NiFeCO complex of carbon monoxide dehydrogenase as a catalytically competent intermediate in the pathway of acetyl-coenzyme A synthesis. *J. Biol. Chem. 266*, 20687−20693.
(41) Bar-Even, A. (2012) Does acetogenesis really require especially low reduction potential? *Biochim. Biophys. Acta 24*, 01055−01059.
(42) Doukov, T. I., Blasiak, L. C., Seravalli, J., Ragsdale, S. W., and Drennan, C. L. (2008) Xenon in and at the end of the tunnel of bifunctional carbon monoxide dehydrogenase/acetyl-CoA synthase. *Biochemistry 47*, 3474−3483.
(43) Segel, I. H. (1975) *Enzyme kinetics: Behavior and analysis of rapid equilibrium and steady-state systems*, Wiley-Interscience, New York.
(44) Hagen, W. R. (2009) *Biomolecular EPR Spectroscopy*, CRC Press, Boca Raton, FL.